Available online at www.sciencedirect.com
SCIENCE DIRECT®
Journal of Nuclear Materials 348 (2006) 256–262
journal of nuclear materials
www.elsevier.com/locate/jnucmat

Simulation study of carbon impurity dynamics on tungsten surfaces exposed to hydrogen ions

Retsuo Kawakami *

Faculty of Engineering, The University of Tokushima, 2-1 Minami-Josanjima, Tokushima 770-8506, Japan

Received 14 June 2005; accepted 26 September 2005

Abstract

The depth profile of C impurity deposited on a W target exposed to H^+ and C^+ impurities at a concentration of C: 0.8% has been calculated in terms of segregation, diffusion and chemical erosion. For the segregation, the Gibbsian model has been used. For the diffusion, a concentration dependent diffusion model (C in WC and/or C) has been utilized. For the chemical erosion, the chemical erosion yield much lower than that for the H–C system has been applied. The calculated depth profiles at 653 K and 913 K are in good agreement with the XPS data. The agreement indicates that there is a significant contribution of segregation, which shifts the maximum C concentration to the top surface in the depth profiles. On the other hand, there are little contributions from diffusion and chemical erosion, which are related closely to formation of WC in the target.

PACS: 34.50.Dy; 34.50.Lf; 64.75.+g; 66.30.Jt; 81.05.Bx

1. Introduction

For a plasma facing material of fusion devices, tungsten (W) is one of the promising candidates because of its low erosion rate and excellent thermal properties [1]. A material mixing between the W target and carbon (C) impurities deposited on the target during the plasma exposure, however, is a matter of concern for the use of W as a plasma facing material [2,3]. This is because the material mixing makes prediction of the net erosion rate which determines the lifetime of the device much more difficult. The C impurity particles are eroded from other walls such as the divertor strike point which is made from C material. Here carbon has been proposed because of its high thermal shock resistance [4]. The eroded C impurity particles are transported through the plasma. Some of them are deposited on the W target. As a result, the original W target performance (e.g. the net erosion rate) will be changed by the C impurity deposition. The change will become more pronounced with increasing plasma exposure. To predict the net erosion rate, therefore, it has been clarified which kind of effects dominate the material mixing and which role the deposited C impurity will play.

In a previous study, an experiment for the exposure of a W target to hydrogen (H) ions with C

* Tel./fax: +81 88 656 7441.
E-mail address: retsuo@ee.tokushima-u.ac.jp

0022-3115/$ - see front matter © 2005 Elsevier B.V. All rights reserved.
doi:10.1016/j.jnucmat.2005.09.019

impurities (less than C: 1.0%) has been performed; in addition a simulation based on the simple binary collision model has been conducted [5,6]. The experimental result showed that a depth profile of C impurities deposited on the target after the exposure was dependent on the C impurity concentration. At a low C impurity concentration (C: 0.1%), at 653 K, the experimental depth profile had a local peak at a depth of around 20 nm, which was in good agreement with the simulation result. From the agreement, it was concluded that the formation of the local peak resulted from recoil implantation of the deposited C impurity due to a synergetic effect of the impinging H ions and C impurity. The synergetic effect means causing different ion surface interaction properties compared to the ones of pure H^+ or C^+ bombardment. Namely, the implanted average range of the deposited C impurity (20 nm) under the simultaneous bombardment by 0.33 keV H^+ and 1 keV C^+ impurity is deeper than the 1 keV C^+ range (4.7 nm) and also sum of the 1 keV C^+ and 0.33 keV H^+ ranges (4.7 nm + 8 nm = 12.7 nm). At a high C impurity concentration (C: 0.8%), the experimental depth profile had a maximum at the top surface and no local peak occurred. This effect could not yet be reproduced by the simulation.

At a target temperature of 913 K (at C: 0.8%), there was also a disagreement between the experimental and simulation results [6,7]. For the simulation, the deposited C impurity drastically expanded into the W target due to thermal diffusion of C in W (which is based on the simple diffusion model). For the experiment, however, such an expansion of the deposited C impurity has not been observed at the high target temperature. Since the previous simulation model cannot fully explain the experimental results at high C impurity concentrations and high target temperatures, therefore, a comprehensive simulation analysis which also includes ion surface interactions and other effects concerning the behavior of the deposited C impurity is required.

In this study, the simulation based on an advanced model developed for explaining the experimental results at target temperatures of 653–913 K at a high C impurity concentration of C: 0.8% has been conducted in terms of thermal effects such as chemical erosion, thermal diffusion and segregation of C impurities deposited on the W target. In order to clearly discriminate between the previous model (by the EDDY simulation [8]) and the advanced model, henceforth, the simulation used in this study is referred to as ERIm (simulation code of ion surface interactions for *ER*osion/deposition and *Im*purity transport). The ERIm simulation is composed of the simple binary collision model [9], a chemical erosion model by Roth et al.'s empirical formula [10], a composition concentration dependent diffusion model [11] and the Gibbsian segregation model [12,13]. This paper discusses each contribution of these effects to the behavior of the deposited C impurities by comparing the ERIm simulation results with the experimental data.

2. Simulation model for behavior of carbon impurity deposited on tungsten

The exposure of W targets to H ions with C impurities at normal incidence is modeled based on experimental conditions of the HiFIT device (see Refs. [5,6] for details). In the experiment, a 1 keV H ion beam consisting mainly of H^{3+} ($\sim$0.33 keV H^+) is produced. C impurities (less than C: 1.0%) consisting mainly of CH_x^+ ($\sim$1 keV C^+) are added to the H ion beam by putting C plates in the ion source chamber. In the simulation, therefore, 0.33 keV H^+ and 1 keV C^+ impurity are assumed as the impinging ions. The hydrogen included in CH_x^+ is neglected because of the too low concentrations. The exposure ion flux Γ and fluence ϕ used in the simulation are the same as the experimental ones: $\Gamma \sim 3 \times 10^{20}\,\mathrm{m^{-2}\,s^{-1}}$ and $\phi \sim 3 \times 10^{24}\,\mathrm{m^{-2}}$. For the target, W at 100 wt% purity is assumed (in the experiment, sintered polycrystalline tungsten at 99.95 wt% is used).

By using ERIm, the behavior of the deposited C impurity is simulated as a result of a dynamic composition change in the target, which results from the deposition of the impinging C impurities and the release/relocation of the W target atoms and/or the deposited C impurities due to collision and thermal processes. Since a detailed explanation of the collision process has already been described throughout, only the key features are presented here (for example, see Ref. [5] for details). In the collision process, movement of the H^+ ions or the C^+ impurities implanted in the W target and the resultant generation of mobile W or C solid atoms (called 'recoil atoms') are simulated based on the simple binary collision model [9]. For the H^+ ions, a retention process is not taken into account: they are assumed to desorb instantaneously after implantation. The movement is followed until their energy is lost below a cut off energy through the elastic

and inelastic energy losses, in the same manner as in TRIM [14]. For the elastic loss, the Kr–C screen potential has been used [15]. For the local inelastic loss due to excitation or ionization in both of the colliding atoms, which occurs in the electronic shells of atoms, the Oen and Robinson model has been applied [16]. For the non-local inelastic loss (or the continuous energy loss) due to the electron gas in the target, the Lindhard and Scharff model has been applied [17] (this energy is lost continuously along the trajectory of mobile particle).

The choice of the cut off energy for mobile particles is very important for the simulation result [18]. In the TRIM manner, the cut off energy is given by the surface binding energy, i.e., the sublimation energy [19]. In this study, based on the TRIM manner, the cut off energy for mobile particles is given by the sum of sublimation energy (7.35 eV for C and 8.90 eV for W) of each solid component weighted by the corresponding relative atomic concentration at the multicomponent target layer: it has a range between 7.35 eV and 8.90 eV. By using this calculation for the cut off energy, the experimental depth profile of C impurity deposited on a W target exposed to 0.33 keV H^+ and 1 keV C^+ at C: 0.1%, which is characterized by a local peak, is confirmed to be reproduced [5]. If the cut off energy is assumed to be 0.1 eV, the calculated depth profile at C: 0.1% shows more spread into the target accompanied by a decrease in its relative concentration, which is in disagreement with the experimental data (not shown here). Details of influence of the cut off energy on the simulation result have also been discussed in Ref. [18].

In the thermal process, three effects on the behavior of the deposited C impurity are newly modeled. The first effect is a chemical erosion (CH_4 release) of the deposited C impurity by the impinging H^+ ions. In this model, C atoms implanted at a depth corresponding to the H^+ penetration range in the target are assumed to be eroded according to a chemical erosion yield Y_{CH_4}. If there are no C atoms at the H^+ penetration range depth, chemical erosion is not assumed to occur. The chemical erosion yield Y_{CH_4} is given by Roth et al.'s empirical formula [10], which is dependent on the energy ($E_i = 0.33$ keV in this study) and flux ($\Gamma = 3 \times 10^{20}$ m^{-2} s^{-1}) of the impinging H^+ ion as well as the target temperature (T varies from 300 K to 1500 K). The empirical formula is well known to reproduce the measured chemical erosion yield of pure C material by H^+ impact, namely the chemical erosion yield in the H–C system.

The second effect on the behavior of the deposited C impurity is thermal diffusion. In this model, the diffusion of C in tungsten carbide (WC) and/or C is assumed as the C impurity diffusion. Rational for this model is the fact that, in the experiment, the exposed W target surface was observed to be covered by WC and/or graphite using XPS [5,6] and that, in the previous simulation, the diffusion of C in W cannot explain the experimental results as described above [6,7]. The diffusion of C in WC and/or C is simulated in the same manner as in TRIDYN/PIDAT [20], in association with the collision process by solving the composition concentration-dependent diffusion equation,

$$\frac{\partial C(x,t)}{\partial t} = D(x,t)\frac{\partial^2 C(x,t)}{\partial x^2} + \frac{\partial D(x,t)}{\partial x}\frac{\partial C(x,t)}{\partial x},$$
$$D(x,t) = f_W(x,t)D_{C\text{–}WC} + f_C(x,t)D_{C\text{–}C}. \quad (1)$$

Here, $C(x,t)$ is the concentration of C at a depth of x and at an exposure time of t, $f_W(x,t)$ and $f_C(x,t)$ are the relative concentrations of W and C, respectively, and $D_{C\text{–}WC}$ and $D_{C\text{–}C}$ are the diffusion coefficients of C in WC and C, respectively. For each diffusion coefficient, $D_{C\text{–}WC} = 9.99 \times 10^{-8}\exp(-4.46 \times e/k_B T)$ m^2/s and $D_{C\text{–}C} = 1.43 \times 10^{-4}\exp(-5.65 \times e/k_B T)$ m^2/s are used (e is the elementary charge, k_B is the Boltzmann constant and T is the target temperature), which were obtained in other diffusion experiments [21,22]. Sublimation is not taken into account. This is accomplished by taking the diffusion flux from the top surface to be zero, i.e., $\partial C(x=0,t)/\partial x = 0$.

The third effect on the behavior of the deposited C impurity is segregation (up-hill diffusion). In this model, Gibbsian segregation is assumed where the driving force is the difference in the chemical potential between the top surface layer and the second layer [12,13]. In analogy to ACAT-DIFFUSE [23], the Gibbsian segregation is simulated in association with the collision process and the other thermal processes by solving the following equation for the relative concentration of C in the W target,

$$\frac{\partial f_C^0(t)}{\partial t} = \frac{M}{a^2} f_C^1(t)\left[\Delta G + k_B T \ln\frac{f_C^1(t)\{1-f_C^0(t)\}}{f_C^0(t)\{1-f_C^1(t)\}}\right],$$
$$\frac{\partial f_C^1(t)}{\partial t} = \frac{M}{a^2} f_C^2(t)\left[\ln\frac{f_C^2(t)\{1-f_C^1(t)\}}{f_C^1(t)\{1-f_C^2(t)\}} - \ln\frac{f_C^1(t)\{1-f_C^0(t)\}}{f_C^0(t)\{1-f_C^1(t)\}}\right],$$
$$\frac{\partial f_C^j(t)}{\partial t} = \frac{M}{a^2} f_C^{j+1}(t)\left[\ln\frac{f_C^{j+1}(t)\{1-f_C^j(t)\}}{f_C^j(t)\{1-f_C^{j+1}(t)\}} - \ln\frac{f_C^j(t)\{1-f_C^{j-1}(t)\}}{f_C^{j-1}(t)\{1-f_C^j(t)\}}\right]. \quad (2)$$

Here, $f_C^0(t)$ is the relative concentration of C at the top surface, $f_C^j(t)$ is the relative concentration of C at jth layer of the bulk target ($j = 1$–500 in this study), and a is the thickness of the layer ($a = 2$ nm). In the equation, ΔG is the segregation energy corresponding to the activation energy in the diffusion, and also, M is expressed by $M = \Theta/RT$, where Θ is the effective diffusion coefficient for the segregation, R is the universal gas constant and T is the target temperature. The contribution of the segregation is characterized by ΔG, Θ, and T. Since these values (ΔG and Θ) for C in W or C in WC are unknown, they are determined by the trial-and-error method in this study so that the experimental results can be reproduced. Details of the segregation model have been described in Refs. [12,13].

3. Results and discussion

3.1. Diffusion, chemical erosion, segregation effects

For the thermal effects of the diffusion, the chemical erosion and the segregation, the ERIm simulation results are described here. If no thermal effects are taken into account, a depth profile of C impurity deposited on a W target exposed to 0.33 keV H^+ and 1 keV C^+ at a high concentration of C: 0.8% is calculated as shown in Fig. 1 (gray curve). In this case, the depth profile has a local peak with a relative C concentration of 70% at a depth of ~17 nm from the top surface. This tendency is quite similar to that for low C impurity concentrations of C: 0.1%, which is well explained by recoil implantation of the deposited C impurities resulting from the ion bombardment as described in detail in Ref. [5]. Even if the diffusion effect of C in WC and/or C is added, there is only little change in the depth profile at target temperatures less than 1500 K in the ERIm simulation (not shown here). This indicates a very important result that, in the ERIm simulation, these target temperatures are essentially diffusion-free. In comparison with the previous simulation result assuming the simple diffusion model of C in W (which shows a deep expansion of the deposited C impurity by the diffusion as described above), there is a clear difference. This mainly results from a difference between the diffusion coefficients used: the diffusion coefficient for C in WC, $D_{C\text{–}WC}$, is much lower than that for C in W, $D_{C\text{–}W}$ (the diffusion coefficient for C in C is the lowest among them). For example, at 913 K, $D_{C\text{–}WC}$ is 2.40×10^{-32} m^2/s, while $D_{C\text{–}W}$ is 4.71×10^{-17} m^2/s (in which $D_0 = 3.15 \times 10^{-7}$ m^2/s and $Q = 1.78$ eV are used [24]). From a comparison between these two simulation results, therefore, the volumetric distribution of the deposited C impurities obtained by using the diffusion model of C in W is found to be significantly suppressed by using the diffusion model of C in WC (and/or C).

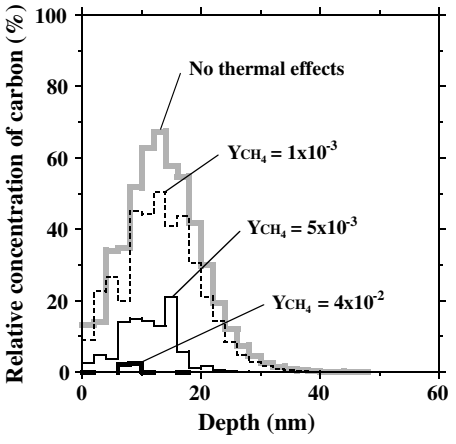

Fig. 1. Dependence of a depth profile of C impurity deposited on a W target exposed to 0.33 keV H^+ and 1 keV C^+ impurity at C: 0.8% (whose total flux and fluence are 3×10^{20} m^{-2} s^{-1} and 3×10^{24} m^{-2}, respectively) on the chemical erosion yield Y_{CH_4}. In the results, the diffusion and segregation models are not included. The gray curve is the result for no thermal effects of the chemical erosion, the diffusion and the segregation.

On the other hand, the chemical erosion effect results in a significant change in the depth profile in the ERIm simulation. According to an empirical formula of chemical erosion in the H–C system by Roth et al. [10], the chemical erosion yield, Y_{CH_4}, as a function of target temperature T under 0.33 keV H^+ bombardment of C with 3×10^{20} m^{-2} s^{-1} has a maximum of 6×10^{-2} at 800 K, and it drastically decreases to zero as the target temperature increases or decreases from 800 K (not shown here). As shown in Fig. 1, therefore, the amount of the deposited C impurities is reduced by an increase in Y_{CH_4} with raising target temperature (300 K $< T <$ 800 K). In particular, at a depth at which the local peak occurs (around ~17 nm in depth), a decrease in the amount of the deposited C impurity is much more pronounced (namely, its relative C concentration drastically is reduced from 70% to 20% by an increase in Y_{CH_4} to 5×10^{-3} with raising target temperature to 700 K). At target temperatures between 700 K and 1000 K, there is no C impurity deposited on the W target because of the

too high chemical erosion yield of $Y_{CH_4} > 5 \times 10^{-3}$. As the target temperature increases from 1000 K, however, the relative C concentration of the local peak increases to 70% because Y_{CH_4} approaches zero, and as a result, the chemical erosion effect is lost. From the ERIm simulation result, therefore, a depth at which the local peak occurs is found to be unchanged by the chemical erosion effect, although there is a significant decrease in its relative C concentration.

For the segregation effect, there is a change in the depth profile different from the chemical erosion effect, as shown in Fig. 2. In the results, ΔG is fixed ($\Delta G = 0.08$ eV) and Θ is increased to $\sim 10^{-17}$ m^2/s regardless of ΔG and T (namely, Θ is independent of ΔG and T). For T, 653 K is assumed. With increasing Θ to 1×10^{-19} m^2/s, there is a decrease in the relative C concentration of the local peak from 70% to 40%. Also, this decrease is accompanied by a shift of the local peak to the top surface (from $\sim$17 nm to $\sim$10 nm in depth). A further increase in Θ (1×10^{-19} m^2/s $< \Theta < \sim 10^{-18}$ m^2/s) results in an increase in the relative C concentration at the top surface. This indicates a very important result that, in the ERIm simulation, no local peak in the depth profile occurs by the segregation effect. At $\Theta > \sim 10^{-18}$ m^2/s, the W target is perfectly covered by the deposited C impurity as shown in Fig. 2. Even if the target temperature becomes higher than 653 K, the tendency in the depth profile resulting from the increase in Θ hardly changes (not shown here). From the ERIm simulation result, therefore, the deposited C impurities are found to be distributed with a maximum at the top surface by the segregation effect.

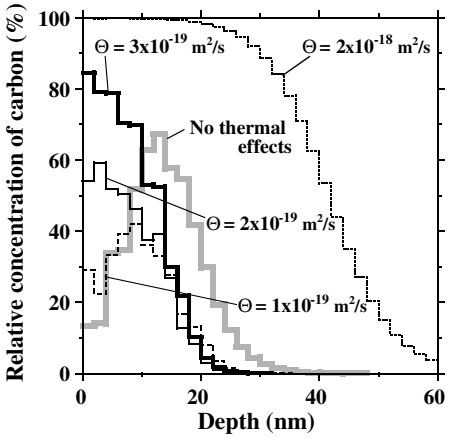

Fig. 2. Dependence of a depth profile of C impurity deposited on a W target exposed to 0.33 keV H^+ and 1 keV C^+ impurity at C: 0.8% (whose total flux and fluence are the same as those in Fig. 1) on the effective diffusion coefficient for the segregation Θ. The segregation energy ΔG is assumed to be 0.08 eV. The target temperature T is assumed to be 653 K. In the results, the chemical erosion and the diffusion models are not included. The gray curve is the same as that in Fig. 1.

3.2. Comparison with experimental results

Based on a change in the depth profile of the deposited C impurities resulting from each contribution of the thermal effects described in the previous subsection, a comparison of the ERIm simulation with the experimental results has been performed as shown in Fig. 3(a) and (b). In this simulation,

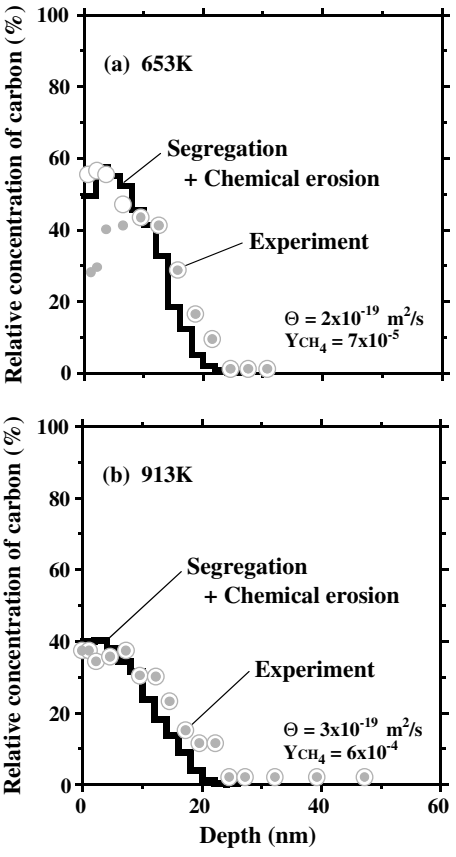

Fig. 3. Comparison of calculated depth profiles of C impurity deposited on a W target at (a) 653 K and (b) 913 K exposed to 0.33 keV H^+ and 1 keV C^+ impurity at C: 0.8% (whose total flux and fluence are the same as those in Fig. 1) with the experimental ones. In the calculated results, the diffusion model is included, but 653 K and 913 K are essentially diffusion-free. The solid and open circles correspond to the experimental data [6]. The former symbol represents formation of WC, and the latter symbol represents sum of WC and C.

the segregation model, the chemical erosion model and the diffusion model are included. For the segregation model, the effective diffusion coefficient for the segregation Θ is assumed to be given from $\Theta = \Theta_0 \exp(-\Delta G \times e/k_B T)$ by analogy with the diffusion coefficient $D = D_0 \exp(-Q \times e/k_B T)$, where D_0 is the material constant and Q is the activation energy. Θ_0 is taken to be $\Theta_0 = 8.3 \times 10^{-19}$ m^2/s and ΔG is assumed to be 0.08 eV. Therefore, Θ at 653 K and 913 K are set to 2×10^{-19} m^2/s and 3×10^{-19} m^2/s, respectively. For the chemical erosion model, the chemical erosion yields Y_{CH_4} is much lower than that given from an empirical formula of chemical erosion in the H–C system by Roth et al. [10]: Y_{CH_4} at 653 K and 913 K are 7×10^{-5} and 6×10^{-4}, respectively. This assumption is based on another experimental result: the chemical erosion from W–C mixed material is suppressed compared with that from pure C material [25]. For the diffusion model, the simulation condition is the same as that descried above (the diffusion of C in WC and/or C).

On the other hand, the experimental results, which are compared with the simulated results in Fig. 3(a) and (b), were obtained by XPS in the HiFIT device (see Ref. [6] for details). In the experimental result, the solid circles represent formation of WC, and the open circles describe the sum of C and WC in the W target (Fig. 3). The experimental results at 653 K and 913 K show that there is a phase of W plus WC at relative C concentrations $< \sim$45%, while there is a phase of C plus WC $> \sim$45%. The phase change in the C-deposited W target by the relative C concentration is consistent with that predicted using the binary alloy phase diagram between W and C [26]. In the ERIm simulation result, no contribution of the binary alloy phase change between W and C is taken into account.

As shown in Fig. 3(a) and (b), the calculated depth profiles at 653 K and 913 K are in good agreement with the experimental ones [6]. In particular, the experimental characteristics that the depth profile has a maximum at the top surface, which decreases with increasing target temperature from 653 K to 913 K, are reproduced. From the agreement, the following results for the behavior of the deposited C impurity are found out. There is a significant contribution of the segregation effect to the behavior of the deposited C impurity at 653 K and 913 K, which results from the fact that there are no local peaks in the depth profiles, as shown in Fig. 3. This indicates that, at the H–C–W system, the segregation effect is dependent on the C impurity concentration (or the amount of the deposited C impurity), because at low C impurity concentrations such as C: 0.1% there is little contribution of the segregation effect [5,6]. From the present study, a detailed reason for the C impurity concentration dependence of the segregation effect cannot be clarified because there is too little information about it in the H–C–W system. For the segregation effect in the H–C–W system, therefore, a detailed investigation has to be performed in terms of the C impurity concentration dependence.

Regarding the diffusion and chemical erosion effects, their contribution is related closely to the formation of WC in the W target. As has already been described above, there is little contribution of the diffusion effect (the diffusion of C in WC and/or C) to the behavior of the deposited C impurities. This result indicates that a deep expansion of the deposited C impurities is significantly suppressed by the formation of WC in the W target, which was identified by XPS in the experiment as shown in Fig. 3. If WC were not formed in the W target, the deposited C impurities would be distributed deeper in the bulk material, according to a previous simulation result showing its deep expansion by the diffusion model of C in W. Identically, the chemical erosion effect hardly contributes to the behavior of the deposited C impurities. This results from ERIm simulations that can well reproduce the experimental data at 653 K and 913 K in the H–C–W system using the chemical erosion yields lower than those expected from the H–C system, as shown in Fig. 3. Therefore, this result indicates that the formation of WC in the W target results in a significant suppression of the chemical erosion at the H–C–W system.

4. Conclusion

Depth profiles of C impurities deposited on a W target exposed to 0.33 keV H^+ with 1 keV C^+ impurity at a concentration of C: 0.8% have been calculated in terms of segregation, diffusion and chemical erosion effects. The calculated results have been compared with XPS data showing formation of WC in the W target. For the segregation, the Gibbsian model has been used. For the diffusion, a composition concentration dependent diffusion model of C in WC and/or C has been utilized. For the chemical erosion, the chemical erosion yield much lower

than that given from the empirical formula in the H–C system has been applied.

The calculated depth profiles, which show no local peak in the depth profiles at 653 K and 913 K, are in good agreement with the experimental data. The agreement indicates that there is a significant contribution of the segregation to the behavior of the deposited C impurities, which results in a maximum C concentration at the top surface. On the other hand, there is little contribution of the diffusion and the chemical erosion effects at the H–C–W system, which is related closely to the formation of WC in the W target.

Acknowledgements

The author is very grateful to Professor Y. Ueda at Osaka University for valuable discussion and suggestion. Also, the author is very thankful to Professor K. Ohya at Tokushima University.

References

[1] K. Krieger, J. Likonen, M. Mayer, R. Pugno, V. Rohde, E. Vainonen-AhlgrenASDEX Upgrade Team, J. Nucl. Mater. 337–339 (2005) 10.
[2] R. Kawakami, K. Ohya, J. Nucl. Mater. 313–316 (2003) 107.
[3] D. Hildebrandt, P. Wienhold, W. Schneider, J. Nucl. Mater. 290–293 (2001) 89.
[4] G. Federici, C.H. Skinner, J.N. Brooks, J.P. Coad, C. Grisolia, A.A. Haasz, A. Hassanein, V. Philipps, C.S. Pitcher, J. Roth, W.R. Wampler, D.G. Whyte, Nucl. Fusion 41 (2001) 1967.
[5] R. Kawakami, T. Shimada, Y. Ueda, M. Nishikawa, Jpn. J. Appl. Phys. 42 (2003) 7529.
[6] T. Shimada, T. Funabiki, R. Kawakami, Y. Ueda, M. Nishikawa, J. Nucl. Mater. 329–333 (2004) 747.
[7] R. Kawakami, T. Shimada, Y. Ueda, M. Nishikawa, J. Nucl. Mater. 329–333 (2004) 737.
[8] K. Ohya, R. Kawakami, Jpn. J. Appl. Phys. 40 (2001) 5424.
[9] W. Möller, W. Eckstein, J.P. Biersack, Comput. Phys. Commun. 51 (1988) 355.
[10] J. Roth, R. Preuss, W. Bohmeyer, S. Brezinsek, A. Cambe, E. Casarotto, R. Doerner, E. Gauthier, G. Federici, S. Higashijima, J. Hogan, A. Kallenbach, A. Kirschner, H. Kubo, J.M. Layet, T. Nakano, V. Philipps, A. Pospieszczyk, R. Pugno, R. Ruggiéri, B. Schweer, G. Sergienko, M. Stamp, Nucl. Fusion 44 (2004) L21.
[11] K.L. Wilson, M.I. Baskes, J. Nucl. Mater. 76&77 (1978) 291.
[12] J. du Plessis, E. Taglauer, Surf. Sci. 260 (1992) 355.
[13] J. du Plessis, G.N. Vanwyk, E. Taglauer, Surf. Sci. 220 (1989) 381.
[14] J.P. Biersack, W. Eckstein, Appl. Phys. 34 (1984) 73.
[15] W.D. Wilson, L.G. Haggmark, J.P. Biersack, Phys. Rev. B 15 (1997) 2458.
[16] O.S. Oen, M.T. Robinson, Nucl. Instrum. and Meth. 132 (1976) 647.
[17] J. Lindhard, M. Scharff, Phys. Rev. 124 (1961) 128.
[18] R. Kosiba, G. Ecke, Nucl. Instrum. and Meth. B 187 (2002) 36.
[19] W. Eskstein, Computer Simulation of Ion–Solid Interaction, Springer, Berlin, 1991, p. 78.
[20] W. Eckstein, V.I. Shulga, J. Roth, Nucl. Instrum. and Meth. B 153 (1999) 415.
[21] H. Bakker, H.P. Bonzel, C.M. Bruff, M.A. Dayananda, W. Gust, J. Horváth, I. Kaur, G.V. Kidson, A.D. LeClaire, H. Mehrer, G.E. Murch, G. Neumann, N. Stolica, N.A. Stolwijk, Diffusion in Solid Metals and Alloys, Springer, Berlin, 1990.
[22] K. Schmid, J. Roth, J. Nucl. Mater. 302 (2002) 96.
[23] T. Takiguchi, M. Ishida, Y. Yamamura, Radiat. Eff. Def. Solids 130&131 (1994) 387.
[24] H. Bakker, H.P. Bonzel, C.M. Bruff, M.A. Dayananda, W. Gust, J. Horváth, I. Kaur, G.V. Kidson, A.D. LeClaire, H. Mehrer, G.E. Murch, G. Neumann, N. Stolica, N.A. Stolwijk, in: H. Mehrer (Ed.), Diffusion in Solid Metals and Alloys, Springer, Berlin, 1990, p. 480.
[25] W. Wang, V.Kh. Alimov, B.M.U. Scherzer, J. Roth, J. Nucl. Mater. 241–243 (1997) 1087.
[26] T.B. Massalski, H. Okamoto, P.R. Subramanian, L. Kacprzak, Binary Alloy Phase Diagrams, 2nd Ed., American Society of Metals, Metals Park, OH, 1990, p. 895.